Fuel Processing Technology 238 (2022) 107523

Contents lists available at ScienceDirect

Fuel Processing Technology

journal homepage: www.elsevier.com/locate/fuproc

hydrothermal co-liquefaction of biomass and plastic wastes into biofuel: Study on catalyst property, product distribution and synergistic effects

Swathi Mukundan [a,b,*], Jonathan L. Wagner [a], Pratheep K. Annamalai [c], Devika Sudha Ravindran [b], Girish Kumar Krishnapillai [b], Jorge Beltramini [d]

[a] Loughborough University, UKRI National Interdisciplinary Centre for Circular Chemical Economy, Department of Chemical Engineering, Epinal way, Loughborough, Leicestershire, LE11 3TU, UK
[b] Cochin University of Science and Technology, Department of Applied Chemistry, University Road, Kalamassery, Kochi 682022, Kerala, India
[c] The University of Queensland, Australian Institute for Bioengineering & Nanotechnology, St Lucia, QLD 4072, Australia
[d] Queensland University of Technology, Centre for Agriculture and the Bioeconomy, Brisbane, QLD 4000, Australia

ARTICLE INFO

Keywords:
Hydrothermal liquefaction
Biomass waste
Plastic waste
Synergy
Biofuels
Nb_2O_5

ABSTRACT

This study reports an efficient conversion route for *prosopis juliflora* (PJ) biomass into high-quality bio-oil through catalytic hydrothermal liquefaction (HTL) process with systematically substituted hydrogen-rich plastic waste 'polypropylene (PP)', and using alumina supported metal oxide (Mo, Ni, W, and Nb) catalysts. The HTL treatments of PJ with PP (0-75 wt.%) were investigated in both sub and supercritical water conditions. An excellent synergy between PP and PJ was observed even in subcritical conditions (97.6% synergy at 340 °C at 25% PP to PJ), while efficient liquefaction of PP alone was observed only in the supercritical conditions. The optimum temperature, and PP substitution were found to be 420 °C and 25% respectively, with 46.5% bio-oil yield, high deoxygenation (65.1%), and carbon recovery (78.9%) when using Nb/Al_2O_3 as the catalyst. An in-depth analysis of physicochemical properties and the bio-oil product distribution with respect to each catalyst and PP/PJ substitution ratio are discussed in detail. Among all, the Nb/Al_2O_3 catalyst performed well with remarkable recyclability up to 10 cycles. The produced bio-oil mixture due to its low oxygen content is very promising to be upgraded to precursors for chemicals and transportation biofuels.

1. Introduction

Due to economic, social, and environmental reasons, research focusing on alternative fuel and chemical sources has gained interest. As reserves of fossil fuel are declining worldwide, combined with an increasing demand for petroleum fuels by emerging economies, the price of conventional fossil fuel shall continue to rise, increasing the risk in energy supply around the world. Furthermore, the environmental damage resulting from the combustion of fossil fuel, by releasing atmospheric pollutants and CO_2, is a contributing factor to global warming [1]. As the only natural-occurring source of renewable organic carbon, biomass represents an essential feedstock to produce chemicals and liquid transportation fuels. The recalcitrant C–C and C–O bonds found in biomass requires a bulk depolymerisation technique to produce bio-oil, a viscous liquid that can be easily processed, stored, and safely 'dropped-in' into the supply chain for large scale chemical conversions in existent refineries [2]. The bio-oil produced from common thermochemical methods consists of a complex mixture of oxygenated compounds (~50% oxygen), which can be upgraded to hydrocarbon fuels and specialty chemicals through proper refining methods such as hydrodeoxygenation, decarboxylation, decarbonylation, isomerisation, hydrogenation, dehydration, etc. [3–7].

In general, bio-oil can be obtained from biomass by pyrolysis and/or hydrothermal liquefaction (HTL) methods. The bio-oil from pyrolysis is highly unstable as a result of its high oxygen content and as a result of vigorous reaction condition which can destroys the natural structure of phenolic compounds [8]. Our earlier investigation on using pyrolysis for valorization of PJ biomass has yielded only 25% bio-oil after removing the aqueous phase [9]. On the other hand, conventional HTL takes place under subcritical water conditions (250 – 373 °C, 4–22 MPa) eliminating the need of a pre-drying step. Under these conditions, water acts both as solvent and as acid-base catalyst, improving the solvation and

* Corresponding author at: Loughborough University, UKRI National Interdisciplinary Centre for Circular Chemical Economy, Department of Chemical Engineering, Epinal way, Loughborough, Leicestershire, LE11 3TU, UK.
E-mail address: s.mukundan@lboro.ac.uk (S. Mukundan).

https://doi.org/10.1016/j.fuproc.2022.107523
Received 21 June 2022; Received in revised form 30 September 2022; Accepted 1 October 2022
Available online 11 October 2022

deoxygenation of intermediate compounds, yielding higher-quality bio-oils compared to pyrolysis [10]. However, supercritical conditions, with temperatures above 380 °C, have been shown to improve glucose conversion, reducing char production compared to subcritical HTL [11]. Besides the carbon rich bio-oil, HTL also yields solid hydrochar, gas products (mostly CO_2) and an aqueous phase, which can be easily separated from the desired bio-oil product.

A potential HTL catalyst must be water-tolerant, display high selectivity towards bio-oil, minimizing char and gas formation. Homogeneous catalysts consisting of base or basic salts such as NaOH, KOH, Na_2CO_3, K_2CO_3 have been intensively utilized for biomass HTL, decreasing the biochar formation and increasing bio-oil yield, however, presenting challenges in separation, extraction, and reusability of the catalyst [12,13]. Heterogeneous catalysts have the advantage of easy separation from the liquid products, improved process economics and energy efficiency. Xu et. al. utilized solid alkaline earth metal catalysts such as hydrotalcite, MgO, and colemanite for woody biomass HTL which improved bio-oil yield and quality [14]. Noble metal catalysts such as Pd/C, and transition metal catalysts based on Ni, W, Co, Mo, and Fe such as Raney nickel, Fe ore, FeS, Ni and Fe metals, CoMo/γ–Al_2O_3, etc. has been also explored for biomass HTL [15–17]. In particular, Ni catalysts produced bio-oil with improved yield and quality due to its hydrogenating property [18,19]. We have previously reported the deoxygenating behavior of Nb_2O_5 catalyst due to its oxophilic nature that can strongly bind with the oxygen groups helping to cleave the C–O bond [9].

As known, biomass tends to be rich in carbon but hydrogen deficient. Hence, incorporating a H-rich co–reactant during the biomass HTL could has the ability to increase the bio-oil yield and quality [20,21]. As such, plastic waste composed of polyolefins (polyethylene, polypropylene, their copolymers and olefinic rubbers) could be a potential co-reactant as contains hydrogen-rich polymers [22–24]. Utilising plastic as a co–reactant not only benefit increasing the bio-oil yield but also benefit mitigating the waste plastic landfilling environmental issue, that could result in an effective waste management strategy. Polypropylene (PP), a non–oxygenated light weight polymer made of long chain molecules (C3H6)n, [25] is one of the most utilized commodity plastics and is present as the largest fraction in the waste-stream [26]. PP at the subcritical hydrothermal liquefaction conditions (350 °C, 20 min, non-catalytic) produced mainly solid (83%) [27]. However, under supercritical water liquefaction has been reported to increase the PP degradation to 91 wt.% oil (80% range naphtha hydrocarbons) at 425 °C and 2−4 h [28]. The same oil yield was achieved at 0.5 – 1 h reaction time when the temperature was increased to 450 °C [28]. This hydrocarbon oil produced from PP can then synergistically improve the biomass conversion and bio-oil quality when is co-liquefied together with biomass [29]. However, until now there has been limited investigation on catalytic liquefaction of biomass with PP and their synergetic interactions on bio-oil yields obtained.

In this study, we aim to investigate the production of renewable hydrocarbons from abundantly available non-food biomass such *as* PJ using the hydrothermal co-liquefaction route. *Prosopis juliflora* (PJ) with a growth rate of 25 km^2/year in India, is an abundant biomass which is resistant to drought and adaptable to different soil types and therefore, is a promising biomass source for biofuel production used in India and other tropical countries [30]. Our target also seeks to elucidate the synergetic effect occurring when polypropylene (PP) wastes are added to PJ in terms of improving the bio-oil yield. The co-liquefaction studies of PJ and PP were conducted over a broad temperature range of 340 °C to 440 °C, using different PJ/PP ratios at 60 min reaction time, where the synergy percentage effect was calculated at each condition.

The first part of this study consisted of the non-catalytic co-liquefaction reactions to optimise the temperature and percentages of PP added to PJ in terms of high bio-oil yield. On the second part, a series of alumina supported metal oxide catalysts were tested for optimum conversion of biomass-plastic mixture. On this account, we firstly aimed to synthesise, characterize, and evaluate the catalytic activity of a series of transition metal oxides (Ni, Mo, W, Nb) supported on γ–Al_2O_3 for the individual and co-liquefaction of PJ and PP. The temperature, percentage of PP added to PJ, effect of catalyst, catalyst: feed ratio, were all optimized in terms of high bio-oil yield. The reaction products from the HTL process (i.e. bio–oil, aqueous phase, gas, and bio– char) are all characterised and optimal process conditions are reported. The regeneration and reusability of the best performed catalyst at the best reaction condition was also studied.

2. Experimental section

2.1. Materials

Ammonium molybdate tetrahydrate (81.0 – 83.0%), nickel (II) nitrate hexahydrate (>98.5%), ammonium metatungstate hydrate (≥85%), niobium pentachloride (99%) were purchased from Merck, India. γ–Al_2O_3 was purchased from BASF chemicals company. Ethanol (99.9%) was purchased from Changshu Hongsheng fine chemicals. *Prosopis juliflora* (PJ) and single-use polypropylene (PP) (polypropylene packaging bags) were collected in and around SSN College of Engineering campus, Chennai, Tamil Nadu, India. Both the PP and PJ waste were cut into small pieces using a blade shredder and sieved to a size of 1mm.

PJ and PP were characterized to understand their composition that plays a vital role in product formation. PJ is a hardwood biomass with 37.9% cellulose, 19% hemicellulose, and 37% lignin [30]. The C, H, N, S and O content of PJ was 48%, 7%, 0%, 2% and 43%, respectively, whereas PP contains 86% C and 14 % H (Table 1). The $(H/C)_{eff}$ of PJ and PP were 0.375 and 1.95, respectively. It is explicit that PP is H-rich whereas PJ is H- deficient. PP contained high amount of volatile matter (96.2%) with less amount of fixed carbon (3%) and negligible ash content. On the other hand, 79% volatile matter, 15.2% fixed carbon (non-volatile carbon) and 5.8% ash content were found in PJ. The high heating value (HHV) of a biomass is highly influenced by the composition of lignocellulosic components, extractives and detrimentally by moisture and ash contents [31]. The HHV of PJ and PP are 20 MJ/Kg and 41 MJ/Kg, respectively. The high HHV of PP is attributed to its high H content and the absence of heteroatoms.

2.2. Characterization of PJ biomass and PP waste

The moisture content, volatile matter, ash content and fixed carbon were analyzed according to ASTM standards E871–82 and E1755–01. Ultimate analysis was conducted using an ELEMENTAR Vario EL III elemental analyzer. Thermogravimetric analysis (TGA) was performed to determine the waste degradation rate using a Shimadzu TGA 50H thermogravimetric analyzer. TGA was performed using 10 mg of waste at a temperature of 30 to 800 °C under 20 °C/min heating rates and held at final temperature for 10 min.

Table 1
Characterization of PJ and PP wastes

	PJ	PP
Carbon (%)	48	86
Hydrogen (%)	7	14
Nitrogen (%)	0	0
Sulphur (%)	2	0
Oxygen (%) (calculated by difference)	43	0
(H/C)eff	0.375	1.95
HHV (MJ/Kg)	20	41
Volatile matter (%)	79	96.2
Fixed carbon (%)	15.2	3
Ash content (%)	5.8	0

2.3. Synthesis and characterization of catalysts

Alumina (γ–Al_2O_3) supported metal catalysts (Mo, Ni, Nb, W) were prepared by simple wetness impregnation method with a nominal metal content of 7 wt.%. The desired amount of aqueous solution of the metal precursor was added to the alumina support and mixed in a rotary evaporator at room temperature for 12 h (In the case of niobium pentachloride, ethanol was used as the solvent due to its decomposition in water). Water was then removed by the rotary evaporator at 50 °C, followed by drying the catalyst overnight at 100 °C, and subsequent calcination at 550 °C for 5 h in a muffle furnace. The catalysts were then labelled as Mo/alumina, Ni/alumina, Nb/alumina, and W/alumina.

The catalyst structural analysis was elucidated by X –ray diffraction (XRD) using Bruker D8 advance with monochromatic Cu Kα radiation (λ = 1.542 Å) at 30 kV and 15 mA with a step size of 0.1 °, for the range of $10° \leq 2\theta \leq 80°$. Nitrogen adsorption-desorption data were obtained at -196 °C using a Micromeritics TriStar II 3020 surface area and porosity analyser. Prior to physisorption measurements, all samples were degassed under vacuum at 200 °C overnight. The specific surface area was determined by applying Brunauer– Emmett– Teller (BET) method and pore volume were calculated from the amount of N_2 adsorbed at P/P_o of 0.99. An Inductively coupled plasma mass spectrometry (ICP–MS) from Thermo Fisher iCAP RQ ICP–MS was used for the bulk elemental analysis. The amount and strength of the catalyst acid sites were characterized using a Micromeritics Autochem II 2920 chemisorption analyzer (TPD-ammonia), fitted with a TCD detector for monitoring NH_3 desorption profile. About 50 mg of sample was preheated for 2 h under the flow of helium gas at 400 °C. Then the sample was saturated by passing 15 vol% NH_3 in He for 1 h at 100 °C. Afterward, was heated from 100 °C to 800 °C at a heating rate of 10 °C/min. In parallel, Pyridine Fourier- Transform Infrared Spectroscopy (FT-IR) was used to determine the nature of the catalyst acid sites. A known amount of pyridine was adsorbed on the 50 mg catalyst at 150 °C. The excess and physiosorbed pyridine were removed by passing N_2 at 150 °C for 30 min and FT-IR was recorded using a Perkin Elmer 200 FT–IR, USA spectrometer at 128 scans and 4 cm^{-1} resolution. A Field Emission Scanning Electron Microscope (FE–SEM) – JOEL 6390LA microscope operated at 30 kV with backscattering (BSE) and Energy Dispersive X–ray Spectroscope (EDAX) detectors was used for characterising the morphology of catalysts. A high-resolution transmission electron microscope (HR-TEM, JOEL/JEM 2100) operated at 200 kV, fitted with an energy dispersive X-ray (EDS) detector was used to find the particle size distribution and metal dispersion over the alumina support. X-ray photoelectron spectrometer (XPS) by Scienta O micron was used to find the oxidation states of Nb_2O_5. The peaks were calibrated by using C 1 s line in the carbon spectra at 284.0 eV as a reference.

2.4. Design of experiments and product analysis

Hydrothermal liquefaction reactions (HTL) were carried out in a 250 ml capacity stainless steel closed high–pressure batch auto–reactor. The reactor was loaded with 15g of feed (biomass and/or PP), a feed: water ratio of 1:8 and pressurized to 5 MPa with nitrogen. After heating to the desired reaction temperature (320 °C to 440 °C, heating rate 10 °C/min), temperatures were maintained for 60 min under constant stirring at 740 rpm. The effect of Mo/alumina, Ni/alumina, Nb/alumina, and W/alumina catalysts on bio-oil yield was studied by varying the catalyst wt. % with respect to feed (1 wt.%, 2 wt.%, 3 wt.%, 4 wt.% and 5 wt.%). It must be noted that the catalysts were not reduced before the reaction. Before dismantling the reactor, the reaction was quenched by removing the heating jackets and immersing the autoclave in an ice water bath. The pressure was released by collecting gases using a Tedlar gas bag. Bio-oil produced from the HTL crude was separated through solvent extraction process using hexane [32]. The contents of the reactor were extracted using hexane as the solvent and transferred into a 250 ml separating funnel where the organic phase was recovered. The organic phase (bio-oil) was subjected to vacuum separation to remove excess hexane. The solid along with the catalyst was collected by filtration and washed with ethanol and dried overnight at 100 °C and analyzed for the coke deposition using an ELEMENTAR Vario EL III elemental analyzer. For the reusability tests, before conducting each test, the catalyst was regenerated by burning off the deposited coke at 400 °C in a muffle furnace [9]. The yield of bio-oil, gas, aqueous phase, and solids, higher heating value (HHV), percentages of deoxygenation in bio-oil, and carbon recovery in bio-oil are evaluated using the formulae given in the electronic supplementary information (ESI). % Synergy and % calculated yields are evaluated using the formulae:

$$\%\text{Synergy} = \frac{\text{Experimental yield} - \text{Calculated yield}}{\text{Calculated yield}} * 100$$

$$\text{Calculated Yield} = (x_{PJ} * y_{PJ} + x_{PP} * y_{PP})/100$$

where x is the mass fraction, y is the % yield, PJ is Prosopis juliflora, and PP is polypropylene.

Gas chromatography–mass spectrometry (GC–MS) was used to analyze the bio-oil, obtained from hydrothermal liquefaction process. An Agilent 7890 GC equipped with an Agilent 7683B auto–injector, a HP–5 column and flame ionization detector (FID) was used. The injector temperature was 250 °C. The column temperature was set at 100 °C and held for 1 min, followed by ramping at 10 °C/min to 200 °C and held for 10 min. A volume of 0.5 μL liquid product was injected in a split mode ratio of 100:0. The average molecular weight of bio-oil was analyzed by gel permeation chromatography (GPC) using a Water GPC 1515 pump system provided with Styragel HT–6E and HT–3 columns linked in series. UV (Waters 2489) and RI (Waters 2414) detectors were used for finding the average molecular weight of bio-oil products. The bio-oil samples were dissolved in 1 mg/ml THF (used as an eluent with a flow rate of 1 ml/min) and filtered using a 0.45 micron filter before analysis. The system was calibrated using the narrow polystyrene standards in the range of M_w 1.3 million Da to 1350 Da.

3. Results and discussion

3.1. Characterization of the synthesized catalysts

Four catalysts (Mo/alumina, Ni/alumina, W/alumina, and Nb/alumina) were studied for the co–liquefaction of PJ and PP. The alumina support had a surface area of 192 $m^2\ g^{-1}$ with a pore volume of 0.49 $cm^3\ g^{-1}$ (Table 2). The metal impregnation over alumina support decreased the surface area to 127, 137, 124, and 139 $m^2\ g^{-1}$, for Mo, Ni, W and Nb catalysts, respectively. Similarly, the deposition of the metal particles in the surrounding pore mouth of alumina decreased the pore volume as expected. The elemental percentage as measured by ICP– MS (Table 2) was 7.3, 6.5, 7.2, and 6.9 for Mo, Ni, W and Nb catalysts, respectively which is in good agreement with the theoretical values (standard deviation = 0.3317).

Table 2 also reports the catalyst acidity measurement by TPD-ammonia. The acid strength is categorized as weak, moderate, and strong depending on the temperature at which ammonia was desorbed from the catalyst [33]. From the table, alumina support exhibits a total acidity of 0.76 mmol/g where about 55% are weak acid sites and 45% moderate acid sites. The metal loading to alumina support increased the total acidity where the highest acidity was found to be for Nb/alumina (1.23 mmol/g). Alumina supported Mo, Ni, and W exhibited 0.92, 0.87 and 0.98 mmol/g total acid sites, respectively. The nature of acid sites (Brønsted/ Lewis) was examined using pyridine FT-IR spectroscopy (Fig. 1a). The characteristic absorption bands at 1425 and 1630 cm^{-1} represented the surface coordinated pyridine molecules with the Lewis (PyL) acid sites whereas, the absorption peak at 1540 cm^{-1} represents the pyridine ion adsorbed on the catalyst Brønsted (PyB) acid sites [33]. The adsorption band at 1480 cm^{-1} is characteristic for a combination of

Table 2
BET surface area, pore volume, pore size, elemental percentage and acid properties of alumina support and Ni/alumina, Mo/alumina, Nb/alumina, and W/alumina catalysts

Support/ catalyst	BET Surface area (m^2g^{-1})[a]	Pore Volume (cm^3g^{-1})	Pore Size (nm)[b]	Elemental percentage (Wt.%)[c]	Number of acid sites (mmol/g)[d]			
					Weak 200 °C–250 °C	Moderate 400 °C–500 °C	Strong >500 °C	Total
Alumina	192	0.49	9.6	–	0.42	0.34	0	0.76
Mo/alumina	127	0.23	4.2	7.3 (Mo)	0.52	0.31	0.09	0.92
Ni/alumina	137	0.25	4.8	6.5 (Ni)	0.43	0.36	0.08	0.87
W/alumina	124	0.24	4.2	7.2 (W)	0.56	0.3	0.12	0.98
Nb/alumina	139	0.27	4.9	6.9 (Nb)	0.54	0.48	0.21	1.23

[a] BET specific surface area.
[b] Pore volume calculated at $P/P_o = 0.99$.
[c] Measured by ICP.
[d] Total acidity by TPD- ammonia.

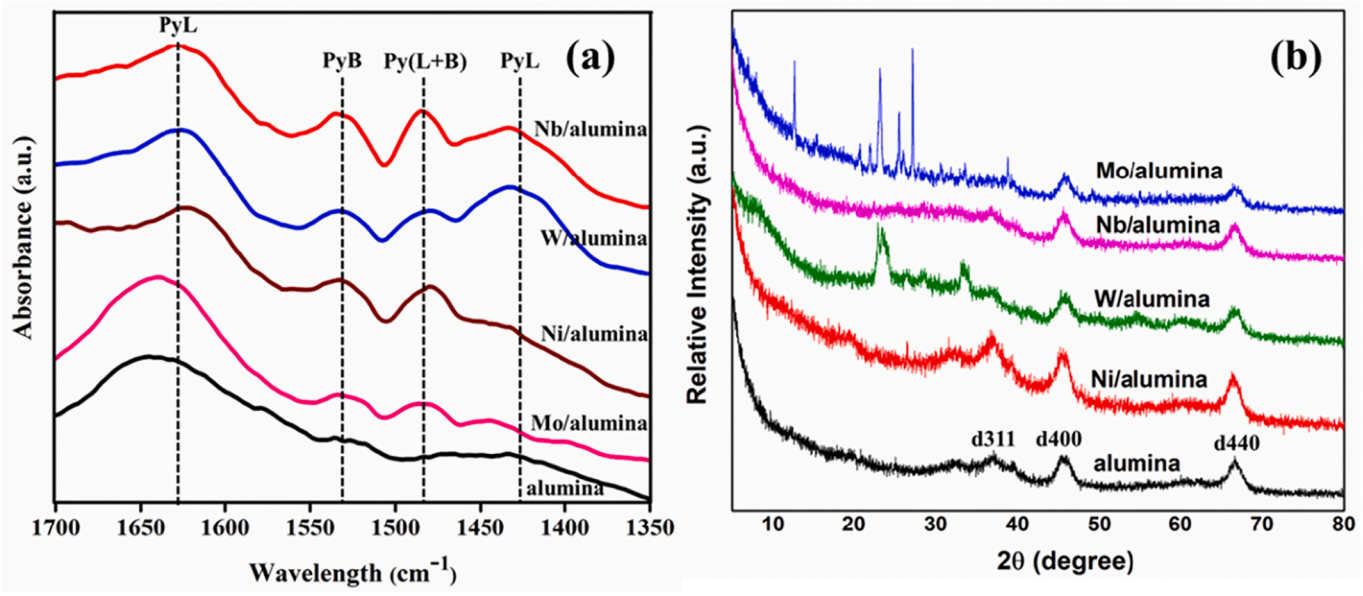

Fig. 1. (a) IR spectra of pyridine adsorbed (b) XRD patterns of alumina support, Ni/alumina, Mo/alumina, Nb/alumina, and W/alumina catalysts

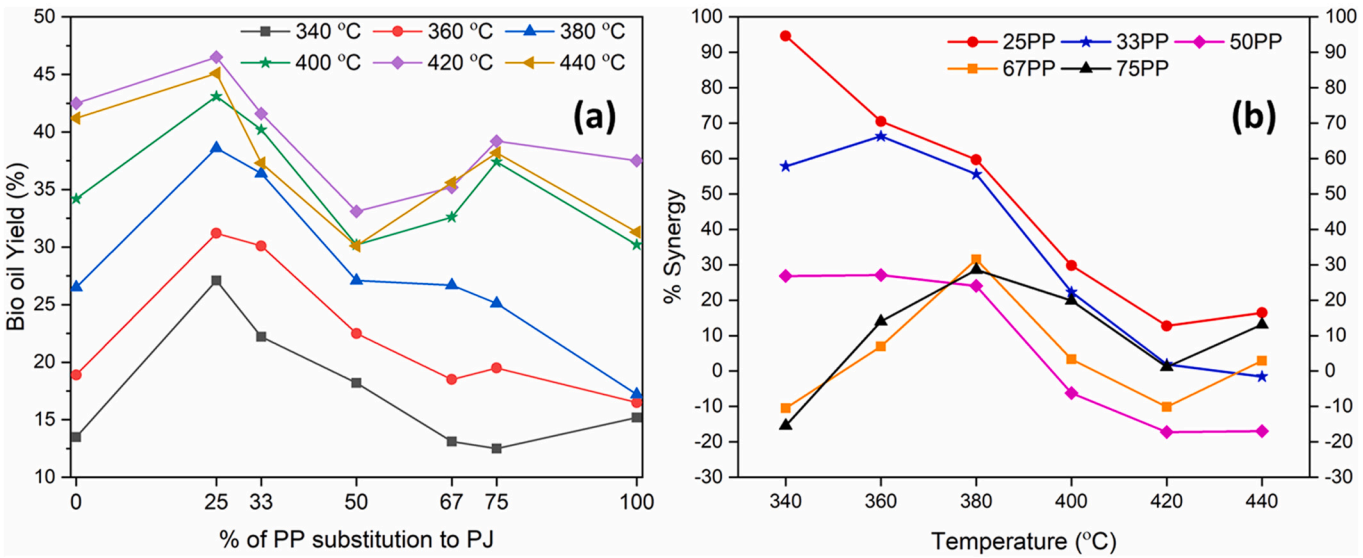

Fig. 2. (a) Overall bio-oil yield (%) and (b) % synergy obtained from the hydrothermal co-liquefaction of PJ and with the addition of PP in different percentage (25%, 33%, 50%, 67%, 75%) respectively, as function of non-catalytic reaction temperature for 60 min

Brønsted and Lewis acid sites (PyL + B). Alumina support exhibits a strong Lewis acidity with a negligible Brønsted acid site. The deposition of metals increased the Lewis and Brønsted acid sites where the highest PyL, PyB and PyL + B was observed with Nb/alumina catalyst in agreement with TPD-ammonia results in Table 1.

The XRD spectra of alumina support in Fig. 1b displayed three main peaks at 2θ = 37.2°, 45.5° and 66.7° corresponding to the d311, d400, d440 reflections of γ–Al_2O_3 (PDF 00–050–0741) [34]. All the supported metal catalysts, apart from exhibiting the signals related to alumina, had additional peaks corresponding to the respective metal oxides (Fig. 1b). The SEM coupled with EDAX images given in Fig. S1 (a-d) in ESI indicated the absence of other elemental impurities.

3.2. Non-catalytic thermal conversion: HTL of PP, PJ, and their blends

Firstly, non-catalytic co-liquefaction of PJ with different percentages of PP added was investigated in a temperature range of 340–440 °C and the bio-oil yields are depicted in Fig. 2a. In the absence of PP, increasing the temperature from 340 °C to 420 °C increased the bio-oil yield from 13.5% to 42.5% with a concomitant decrease in solid residues (Fig. S2 in ESI). Increasing temperature stimulates the conversion of organic compounds into bio-oil, gaseous products, and other water-soluble compounds. While further increasing the temperature to 440 °C, the yield of bio-oil slightly dropped (from 42.5% to 41.2%), because of thermal cracking of bio-oil compounds following in an increase of gaseous product from 24.4% at 420 °C to 28.9% at 440 °C (Fig. S2 in ESI).

On the other hand, HTL of PP alone, at the subcritical conditions (below 380 °C) yielded mainly 58.6%, 50.2% and 47.4% solid residue products, with an oil yield of 15.2, 16.5 and 17.2% at 340 °C, 360 °C, and 380 °C, respectively which is comparable to the findings by Savage. et. al and Biller. et. al. [20,27], where it was claimed that at subcritical reaction condition, PP degradation was low due to the insufficient number of reactive active sites for dehydration [27]. The appreciable oil yields started at the supercritical condition, where oil yield of 30.2 % was obtained at 400 °C, reaching a maximum yield at 420 °C (37.5%) with further decrease to 31.3% at 440 °C, similar behavior as observed with PJ. Concurrently, the solid products decreased from 58.6% (at 340 °C) to 20.2% at 420 °C, owed to the supercritical water that stabilizes the radicals minimizing coke formation [28].

When adding 25% PP during liquefaction of PJ, a substantial increase in bio-oil yield at 340 °C (13.5% to 27.1%) was obtained. This yield is 97.6% higher than the calculated yield based on a weighted average of PJ and PP yields (Fig. S3a in ESI) and suggests a significant synergy occur during the co-conversion of the two materials. Similarly, the solids decreased to 30.2%, compared to 47.3% when PJ alone was used at 340 °C. Subsequently, a gradual increase in bio-oil yields up to 46.5% at 420 °C was observed, representing about a 12.8% bio-oil yield improvement for all the non-catalytic HTL reaction conducted in this study. It is known that during HTL, decomposition through free-radical formation is more prevalent and the PP is known for the rapid formation of (more stable tertiary) free radicals upon C-H cleavage during thermal decomposition [35]. These free-radicals from PP are expected to bond with the oxygen radicals from biomass, thereby promoting the cleavage of the oxygenated groups from biomass enhancing the oil fraction formation [36]. As such, the bio-oil yield dropped to 45.1% when the temperature was further increased to 440 °C.

As can be seen in Fig. 2a, a further increase in PP substitution to 33%, 50%, 67% and 75% respectively, although indicated good synergy (Fig. 2b) and bio-oil yield improvement, when compared to the anticipated calculated value, the amount of solid products formation increased resulting in poor bio-oil yield when compared to the yield obtained with 25% PP added to PJ. The maximum bio-oil yield at 25% PP implies that only a small amount of PP is sufficient to be added to generate enough radicals to break down biomass. Based on the data obtained from the non–catalytic HTL tests performed, 420 °C was selected as an optimum HTL reaction condition for further studies under the presence of a catalyst.

3.3. Catalyst thermal conversion: HTL of PP, PJ, and their blends

The alumina supported transition metal oxide catalysts were screened for the co-liquefaction of PJ and PP at 420 °C, then compared to the non-catalytic reaction results (Fig. 3a). Initially, to distinguish the role of metals on the bio-oil composition and production, a blank experiment for the co-liquefaction reaction was carried out using only alumina support as catalyst.

At 420 °C, HTL of PJ on alumina as a catalyst, resulted in 40.2% bio-oil yield, found to be 5.4% lower than that obtained from the non-catalytic reaction. Even with the addition of 25% and 33% PP to PJ, similar decrease in the bio-oil yield was observed (7.4%, 4.8% decrease in bio-oil yield at 25%, 33% PP addition, respectively). On the contrary, further increase in the PP % to 50%, 67% and 75% improved the bio-oil yield by 9.1%, 13.1%, and 11.7%, respectively.

In an interesting approach, where HTL reaction was carried out using PP only, a 32% improvement in the bio-oil yield was observed, confirming a positive effect when alumina is present compared to the non-catalytic reaction. As PP comes in contact with alumina support Lewis acid sites, the degradation of PP to lower molecular weight compounds increases sharply [37]. As is known, the catalytic degradation of PP occurs via an ionic mechanism through two steps. The first step is the abstraction of hydride ion from the hydrocarbon polymer which is promoted by the Lewis acid sites of the alumina, where the second step is the formation of a variety of hydrocarbon isomers due to isomerization reaction and β–scission [35,38]. From these results, it can be inferred that alumina as a catalyst is very promising for PP conversion in terms of high oil yield as compared to PJ.

With the presence of transition metal oxides, the conversion of PJ alone, contrastingly, showed an increase in the bio-oil yield for all the catalysts tested in the order of Nb > Ni > Mo > W (22.6%- Nb, 3.8%- Ni, 1.7 %- Mo, and %- W improvement when compared to non-catalytic conversion). Similarly, when PP alone was used, the performance of the supported metal catalysts was exceptional increasing oil yield to 73.3%, 65.3%, 57.3%, and 54.6% for Nb/alumina, Ni/alumina, Mo/alumina, and W/alumina, respectively when compared to the non-catalytic conversion.

The bio-oil yields obtained for the co-liquefaction experiments with 25%, 33%, 50%, 67%, and 75% PP substitution and at 420 °C, are then compared with the calculated anticipated value based on the corresponding individual conversion from the weight fractions of PP and PJ as shown in Fig. S4 (a-e) in ESI. At 25% PP addition, an excellent synergy between PJ and PP was observed producing a high bio-oil yield of 59.4% for Nb/alumina catalyst. The bio-oil yields obtained when using the other catalysts were 47.8%, 48.7% and 49.6% for Mo/alumina, W/alumina, and Ni/alumina, respectively. Evidently, the presence of a metal oxide catalyst improves the overall conversion of solid feed, suppressing gas product formation, thereby increasing the liquid hydrocarbons yield (Fig. 3b) [21]. An increase in the aqueous phase yield was noted, indicating the extraction of organic compounds into the aqueous phase and due to increased deoxygenation reactions, such as demethoxylation in the presence of catalyst. These results suggest that adding 25% PP to PJ is an optimum value in terms of high bio-oil yield (both in the case of catalytic and non– catalytic conversion).

As established Nb/alumina catalyst was found to be the best choice in terms of bio– oil yield, then it was decided to further optimize the catalyst weight percentage for the 25% PP added to PJ during HTL reaction by investigating the bio-oil yield obtained when a catalyst loading of 1, 2, 3, 4, and 5 wt.% was used. At the low catalyst loading of 1 wt.%, 24% solids, 42% bio-oil, 17.2% aqueous phase and 16.8% gases were produced. The low bio-oil liquid yield obtained can be attributed to the limited catalyst amount used to drive the conversion to oil, therefore, the oil production is rivalled by gas and solid product formation. The

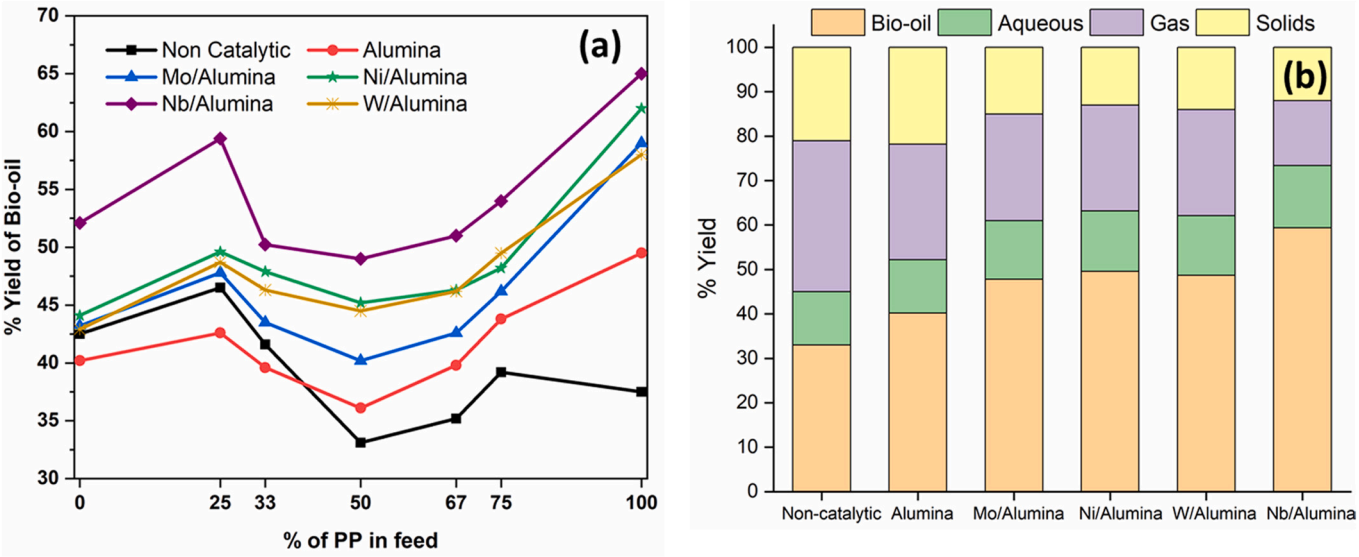

Fig. 3. (a) Effect of different catalyst on bio-oil yield for the hydrothermal liquefaction of prosopis juliflora (PJ) and with the addition of polypropylene (PP) in different percentage (0%, 25%, 33%, 50%, 67%, 75% and 100%). (b) Yield (%) of bio-oil, aqueous, gas and solids produced with different catalysts at 25% PP addition. (Catalyst = 2 wt. %, Temperature = 420°C, time = 60 min)

increase in catalyst load from 1 wt.% to 2 wt.%, increased the bio-oil yield to 59.4%, while decreasing solid residue formation by 50% (24%–1 wt.% to 12%–2 wt.%) suggesting the effective conversion of organic compounds into HTL products. Further increasing catalyst loading results in an increase in gas phase formation due to further decomposition of low molecular weight hydrocarbons from bio-oil due to strong catalyst acidity. Gradual increase in solid residue formation was also observed at increased catalyst load which would have been due to the re–polymerization of oil intermediates. Hence, 2 wt.% of Nb/alumina catalyst was the optimum loading for the HTL reactions.

3.4. Bio– oil product analysis

Table 3 shows the physicochemical properties of the bio-oils obtained from the non-catalytic and catalytic HTL tests conducted at 420 °C and with 25% PP addition to PJ biomass. The 75% PJ–25% PP blend feedstock contains 55.7% C and 6.4% H with a net hydrogen to carbon ratio $(H/C)_{eff}$ of only 0.38. C and H in the bio-oil obtained from the non-catalytic HTL was 59.5% and 6.7%, respectively, with an increased $(H/C)_{eff}$ of 0.52. Due to the low bio-oil yield and carbon loss through solid and gas products, only 40.1% carbon was recovered into the oil phase. Evidently, the catalytic runs produced much improved bio-oil in terms of $(H/C)_{eff}$ and carbon recovery as can be seen in Table 3. With Nb catalyst, about 79% carbon was recovered to the oil phase with $(H/C)_{eff}$ as 1.13.

Table 3
Physicochemical properties of bio-oil obtained with Mo/alumina, W/alumina, Ni/alumina, and Nb/alumina catalysts for the hydrothermal co–liquefaction of 25% PP. (75% *prosopis juliflora* (PJ) and 25% polypropropylene (PP)). (Catalyst: feed = 1: 50, Temperature = 420 °C, time = 60 min).

	75% PJ-25% PP blend feedstock	Non-catalytic	Mo	Ni	W	Nb
C (%)	55.7	59.5	69.0	71.0	68.0	74.0
H (%)	6.4	6.7	8.3	8.4	8.2	9.1
N (%)	0	0	0	0	0	0
S (%)	1.7	1.5	1.1	1.2	0.9	0.1
O (%)	36.2	32.3	21.6	19.4	22.9	16.8
$(H/C)_{eff}$	0.38	0.52	0.96	1.00	0.93	1.13
% Deoxygenation in bio-oil	–	16.5	51.8	58.0	48.2	65.1
% Carbon recovery in bio-oil	–	40.1	59.2	63.2	59.5	78.9
Bio-oil average molecular weight (Mw), g/mol	–	692	526	424	582	368
HHV (MJ/Kg)	23.54	25.64	31.91	32.97	31.31	35.08

In terms of oxygen, the non-catalytic bio-oil contained 32.3% oxygen corresponding to 16.5% bio-oil deoxygenation when compared to the feed. During the catalytic runs, up to 65.1% deoxygenation was achieved with Nb/alumina catalyst as occurrence of several reactions during the HTL, which is discussed in the following sections. It must be also noted that 1.7% sulphur was present in the feed and brought down to 0.1% when Nb/alumina catalyst was used for the HTL reaction, supporting the evidence that Nb is an efficient catalyst for desulphurization reactions as well [39]. Nb catalysts has been reported prominent for dehydration due to its Lewis and Bronsted acid sites [40]. Higher heating value (HHV) is the heat produced upon complete combustion is one of the vital properties of bio-oil which is influenced by factors such as % of heteroatom, H/C ratio, etc. The HHV of the feedstock was 23.54 MJ/Kg which was also improved while employing a catalyst and a maximum of 35.08 MJ/Kg was observed with Nb catalyst.

Overall, by comparing the bio-oil properties, Nb/alumina catalyst performed exceptional in terms of improving bio-oil properties such as HHV and in terms of % deoxygenation and % carbon recovery.

With respect to product distribution, the bio-oil obtained from the catalyzed HTL of PP alone at 420 °C was analyzed by GC-MS and *n*–paraffin, *i*–paraffin, olefin, naphthene and aromatics hydrocarbons in the range of C_7 to C_{18} were observed. The main products identified from GC-MS were methyl cyclohexane (C_7H_{14}), methylhexane (C_7H_{16}), 2,4–dimethyl–1–heptene (C_9H_{18}), 2– decene–2,4–dimethyl ($C_{12}H_{24}$), hexyl cyclohexane ($C_{12}H_{24}$), 3–ethyl–5–methyl–1–propyl cyclohexane ($C_{12}H_{24}$), 1,4–dicyclohexylbutane ($C_{16}H_{30}$), undecylcyclohexane ($C_{17}H_{34}$), pentadecene ($C_{17}H_{34}$), and dodecylcyclohexane ($C_{18}H_{36}$). The aromatic product includes toluene (C_7H_8), trimethylbenzene (C_9H_{12}) and xylene (C_8H_{10}). Escola et al. has reported the formation of C_1-C_5 range products with highly acid catalyst formed by the end-chain scission reaction [41]. The other two conversion pathways of PP are: (i) oligomerization of the produced olefinic gas products, and (ii) the

cracking reactions occurring at random position of the polymer chain [41].

The composition of the obtained bio-oils from PJ and the co-liquefaction studies with different PP concentrations were quantified also by GC-MS analysis and categorized into seven major classes. (i) guaiacolics, (ii) aromatic hydrocarbons, (iii) acids, aldehydes, and ketones (iv) alkyl phenolics, (v) catechols, (vi) naphthalene oligomers, and (vii) alkanes. The detected naphthalene compounds and undetected large naphthalene molecules were considered as naphthalene oligomers. Biomass undergoes decomposition and de–polymerization during the initial HTL process temperature which further produce smaller molecules through addition, cracking, hydrogenation, oxidation and nucleophilic reactions [42].

Fig. 4 shows the selectivity towards bio-oil components for the non-catalytic and catalytic HTL runs with 25% PP in PJ at 420 °C for 60 min and 2 wt.% catalyst. The non– catalytic HTL of 25% PP blend produced guaiacolics (42%), followed by acids, aldehydes, and ketones (26%). 12% of completely oxygen-free compounds: aromatic hydrocarbons were produced as a result of the deoxygenation reaction taking place under non-catalytic hydrothermal condition. It was noticed that 6% alkyl phenolics, 6% catechols, and 8% naphthalene oligomers were the other product classes identified (Fig. 4). During the HTL reaction, repolymerization and condensation reactions occur that produce oligomers. There were no alkanes detected from GC– MS. As it is well known, biomass constitutes cellulose, hemicellulose, and lignin components. The presence of major derivatives compounds from lignin in the bio– oil can be attributed to the more solubility of cellulose derived compounds in water.

During the catalytic HTL reaction of 25% PP added to PJ, interesting results were observed. The guaiacolics selectivity decreased from 42% in case of non-catalytic to 32%, 34%, 33% and 29%, when the Mo, Ni, W and Nb catalysts are used, respectively. There was a simultaneous increase in the yield of aromatic hydrocarbons which can derive to the inference that the deoxygenation of guaiacolics takes place in the presence of metal oxide catalysts to produce aromatic hydrocarbons. Moreover, the bio-oil average molecular weight was calculated by GPC and results shown in Table 3. The non-catalytic HTL of 25% PP blend produced bio-oil with an average molecular weight of 692 g/mol. Whereas, during the catalytic HTL, the average molecular weight

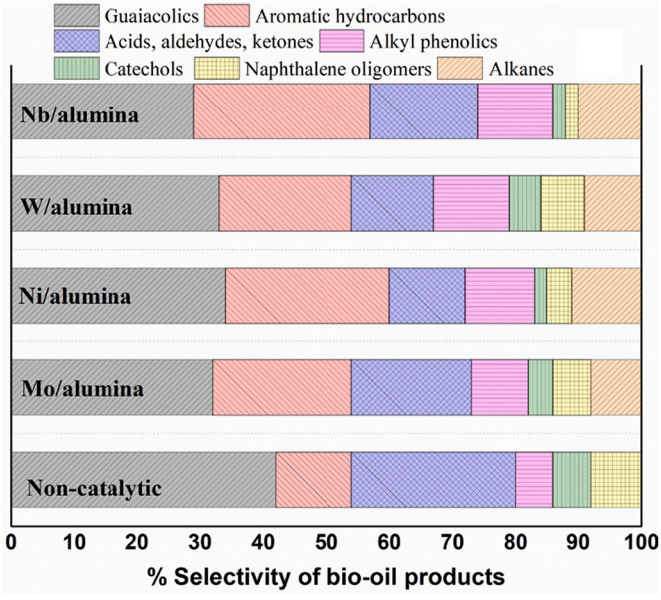

Fig. 4. % Selectivity of products in bio– oil for the hydrothermal liquefaction of 1:3 (PP: PJ) with non-catalytic and Mo/alumina, Ni/alumina, Nb/alumina, and W/alumina catalysts (Catalyst: feed = 1: 50, Temperature = 420 °C, time = 60 min).

decreased to 526, 582, 424 and 368 g/mol for alumina supported Mo, Ni, W and Nb catalysts, respectively. This indicates the effective cleavage of C–C bonds in biomass in the presence of catalyst. It has been reported that Nb_2O_5 possess exceptional hydrogenolysis activity by selectively cleaving $C_{aromatic}$ – C lignin bonds, while suppressing hydrogenation reaction, when compared to other supports such as ZrO_2, Al_2O_3, TiO_2 [43]. The exceptional dehydration capacity of Nb catalyst can be ascribed to the oxophilic nature of Nb_2O_5 (XPS spectra in Fig. S5 in ESI) that possess an unique dehydration potential due to the strong interaction between the Nb^{5+}/Nb^{4+} and the oxygen atom of the guaiacol molecule [44]. Xia. et al. reported that the C– O bond cleavage in tetrahydrofuran ring performed by Nb– O– Nb is the result of an increase of acidity of NbO_x that favors an increase in the rate of dehydration reaction [45]. The direct conversion of biomass derived carbohydrates and glucose involves the dehydration to produce hydroxymethylfurfural and Nb based catalysts has been reported to be promising for this direct conversion [46,47]. Additionally, the selectivity to acids, aldehydes, and ketones, were lesser during catalytic HTL when compared to the non–catalytic conversion (from 26%– non catalytic to 19%, 12%, 13%, and 17% with Mo, Ni, W and Nb, respectively).

The decrease in selectivity to this group of compounds along with the associated increase in CO_2 and CO gases infer that decarboxylation and decarbonylation reactions of the acid, aldehyde and ketone groups were taking place [48]. The decarboxylation and decarbonylation reactions are accompanied by the formation of CO_2 and CO, respectively which can be observed in the gas products (Fig. S6 in ESI).

In contrast, catalytic HTL increased the selectivity to alkyl phenolics when compared to non–catalytic HTL (from 6%– non catalytic to 9%, 11%, 12%, and 12% with Mo, Ni, W and Nb, respectively). Alkylation of guaiacol aromatic ring is a common reaction that occurs in the presence of an acidic catalyst and an alkyl source under hydrothermal conditions [49]. Demethylation and demethoxylation of guaiacol produces CH_4 and CH_3OH, where this methyl group could alkylate the aromatic ring producing alkylated products as a result of the catalyst acidity (Table 1) [5]. The next class of product compound, catechols and naphthalene oligomers showed a yield decrease due to the presence of catalyst. The catechols and naphthalenes have been reported to produce coke through condensation reactions, [50] therefore, the decrease in selectivity to naphthalene oligomers and catechols implies the decomposition of these coke precursors in the presence of catalyst. The presence of acidic catalyst also promotes the formation of gases from PP by the end-chain cleavage mechanism. A complete deoxygenation of guaiacolics and alkylphenolics results in the formation of aromatic hydrocarbons and alkanes as can be seen in Fig. 4.

3.5. Nb_2O_5/alumina: catalyst regeneration and reusability

The efficiency of the Nb_2O_5/alumina catalyst was further investigated for its catalytic reusability. After reaction, the catalyst was separated from the reaction mixture and regenerated by burning off the deposited coke at 400 °C in a muffle furnace. The reusability tests were then conducted using the same reaction conditions as the fresh one. There is a catalyst loss of about ~3.4% every time which was compensated from a fresh batch. The yield of bio-oil, aqueous phase, biochar, and gases from each reaction were quantified and the corresponding % deoxygenation and carbon recovery to bio-oil phase were calculated, and the data presented in Fig. 5. The catalyst performed remarkably up to 10 reaction cycles maintaining a high bio-oil yield with a marginal decrease (59.4% yield–1st cycle to 55.2%–10th cycle). The decrease in bio-oil yield was also followed by a decrease in the % carbon recovery to bio-oil from 78.9% in 1st cycle to 75.8% in 10th cycle which is not a significant loss. An increase in the biochar yield was observed from 12% to 15% after 10th cycle. These results demonstrate that the catalyst is promising for reusability.

For a comparison, the catalyst retrieved after first cycle was tested for reusability without regeneration (burning coke at 400 °C), and as

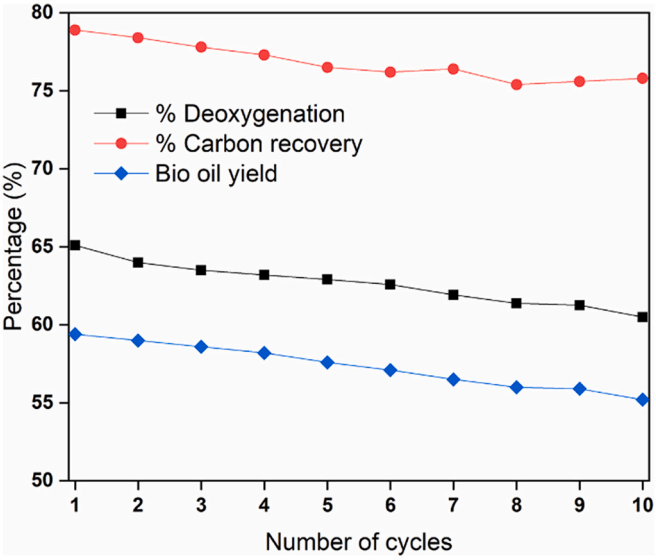

Fig. 5. Catalyst reusability study: Yield of products (bio-oil, aqueous, gas and char), the degree of deoxygenation (%) in bio-oil and % carbon recovery in bio-oil with Nb/alumina catalyst for the HTL of (1:3) PP: PJ blends up to 10 reaction cycles.

expected the bio-oil yield decreased from 59.4% to 55.6% whereas gas and biochar yield sharply increased. This is due to the coke deposited on the catalyst surface covering Nb_2O_5 active site, therefore, hindering the contact of reactant with the catalyst active acid species. Therefore, the regeneration of the catalyst was essential after every reaction cycle. The catalyst deactivation during HTL reactions have been reported to occur due to multiple factors such as leaching of active metals to the liquid medium,[51] catalyst coking that blocks the pores and masks the active sites,[51] the presence of high concentration of hetero atoms in the feed, [52] etc. On the other hand, ɣ-alumina tend to deactivate in hot water and change phase to aluminium oxide hydroxide (boehmite) that also contains Lewis acid sites [53]. However, this phase change could lead to catalyst deactivation [54].

4. Conclusions

In this study, PJ was converted to bio-oil by hydrothermal liquefaction process that can be further upgraded to biofuels or platform chemicals. To improve the bio-oil yield and quality, a hydrogen rich co-reactant PP and solid acid catalysts were employed. The synergistic interaction between the PJ and PP (25% PP substitution to PJ) at HTL reaction temperature of 420 °C increased the oil yield to 46.5% from 42.5% obtained when using PJ alone. Among the catalysts, Nb based catalysts showed high selectivity and efficiency for deoxygenation of liquid biomass compounds resulting in high hydrocarbons with reduced oxygen content, making them very suitable for conversion into transportation platform fuels. Nb/Al_2O_3 was reasonable stable up to 10 reaction cycles. This strategy could be useful both for efficient valorisation of PJ and recycling of PP waste into high value fuels and chemicals which could potentially benefit to Indian farmers, rural industries-based bioeconomy, and municipalities strategies for plastic waste management.

Funding

This research did not receive any specific grant from funding agencies in the public, commercial, or not-for-profit sectors.

CRediT authorship contribution statement

Swathi Mukundan: Investigation, Writing – original draft, Supervision, Funding acquisition. **Jonathan L. Wagner:** Writing – review & editing, Conceptualization. **Pratheep K. Annamalai:** Writing – review & editing, Conceptualization. **Devika Sudha Ravindran:** Formal analysis. **Girish Kumar Krishnapillai:** Writing – review & editing, Supervision. **Jorge Beltramini:** Writing – review & editing, Supervision.

Declaration of Competing Interest

The authors declare that they have no known competing financial interests or personal relationships that could have appeared to influence the work reported in this paper.

Data availability

Data will be made available on request.

Acknowledgements

Dr. SM thankfully acknowledge the University Grants Commission-Dr. D. S. Kothari Postdoctoral Fellowship Scheme for sponsoring the research. The first author sincerely appreciates the facilities provided by SAIF STIC, Cochin University of Science and Technology, Kochi.

Appendix A. Supplementary data

Supplementary data to this article can be found online at https://doi.org/10.1016/j.fuproc.2022.107523.

References

[1] B. Obama, The irreversible momentum of clean energy, Science 355 (2017) 126–129, https://doi.org/10.1126/science.aam6284.
[2] R. Ghadge, N. Nagwani, N. Saxena, S. Dasgupta, A. Sapre, Design and scale-up challenges in hydrothermal liquefaction process for biocrude production and its upgradation, Energy Conv. Manage.: X 14 (2022), 100223, https://doi.org/10.1016/j.ecmx.2022.100223.
[3] S. Mukundan, L. Atanda, J. Beltramini, Thermocatalytic cleavage of C–C and C–O bonds in model compounds and kraft lignin by $NiMoS_2$/C nanocatalysts, Sustain. Energy Fuels 3 (2019) 1317–1328, https://doi.org/10.1039/C8SE00576A.
[4] S. Mukundan, M.A. Wahab, L. Atanda, M. Konarova, J. Beltramini, Highly active and robust Ni–MoS 2 supported on mesoporous carbon: a nanocatalyst for hydrodeoxygenation reactions, RSC Adv. 9 (2019) 17194–17202, https://doi.org/10.1039/C9RA02143D.
[5] S. Mukundan, M. Konarova, L. Atanda, Q. Ma, J. Beltramini, Guaiacol hydrodeoxygenation reaction catalyzed by highly dispersed, single layered MoS_2/C, Catal. Sci. Technol. 5 (2015) 4422–4432, https://doi.org/10.1039/C5CY00607D.
[6] W. Wanmolee, J.N. Beltramini, L. Atanda, J.P. Bartley, N. Laosiripojana, W.O. S. Doherty, Effect of HCOOK/ethanol on Fe/HUSY, Ni/HUSY, and Ni–Fe/HUSY catalysts on lignin depolymerization to benzyl alcohols and bioaromatics, ACS Omega 4 (2019) 16980–16993, https://doi.org/10.1021/acsomega.9b02413.
[7] S. Mukundan, D. Boffito, A. Shrotri, L. Atanda, J. Beltramini, G. Patience, Thermocatalytic hydrodeoxygenation and depolymerization of waste Lignin to oxygenates and biofuels in a continuous flow reactor at atmospheric pressure, ACS Sustain. Chem. Eng. 8 (2020) 13195–13205, https://doi.org/10.1021/acssuschemeng.0c02102.
[8] J. Nallasivam, P.F. Prashanth, R. Vinu, Chapter 4 - Hydrothermal liquefaction of biomass for the generation of value-added products, in: S. Varjani, A. Pandey, M. J. Taherzadeh, H.H. Ngo, R.D. Tyagi (Eds.), Biomass, Biofuels, Biochemicals, Elsevier, 2022, pp. 65–107.
[9] S. Mukundan, G. Sriganesh, P. Kumar, Upgrading Prosopis juliflora to biofuels via a two-step pyrolysis–Catalytic hydrodeoxygenation approach, Fuel 267 (2020), 117320, https://doi.org/10.1016/j.fuel.2020.117320.
[10] A.R.K. Gollakota, N. Kishore, S. Gu, A review on hydrothermal liquefaction of biomass, Renew. Sust. Energ. Rev. 81 (2018) 1378–1392, https://doi.org/10.1016/j.rser.2018.08.047.
[11] C. Promdej, Y. Matsumura, Temperature effect on hydrothermal decomposition of glucose in sub-and supercritical water, Ind. Eng. Chem. Res. 50 (2011) 8492–8497, https://doi.org/10.1021/ie200298c.
[12] J. Akhtar, S.K. Kuang, N.S. Amin, Liquefaction of empty palm fruit bunch (EPFB) in alkaline hot compressed water, Renew. Energy 35 (2010) 1220–1227, https://doi.org/10.1016/j.renene.2009.10.003.

[13] A. Liu, Y. Park, Z. Huang, B. Wang, R.O. Ankumah, P.K. Biswas, Product identification and distribution from hydrothermal conversion of walnut shells, Energy Fuel 20 (2006) 446–454, https://doi.org/10.1021/ef050192p.

[14] L. Nazari, Z. Yuan, S. Souzanchi, M.B. Ray, C. Xu, Hydrothermal liquefaction of woody biomass in hot-compressed water: Catalyst screening and comprehensive characterization of bio-crude oils, Fuel 162 (2015) 74–83, https://doi.org/10.1016/j.fuel.2015.08.055.

[15] M. Scarsella, B. de Caprariis, M. Damizia, P. De Filippis, Heterogeneous catalysts for hydrothermal liquefaction of lignocellulosic biomass: A review, Biomass Bioenergy 140 (2020), 105662, https://doi.org/10.1016/j.biombioe.2020.105662.

[16] X. Ding, S. Mahadevan Subramanya, K.E. Waltz, Y. Wang, P.E. Savage, Hydrothermal liquefaction of polysaccharide feedstocks with heterogeneous catalysts, Bioresour. Technol. 352 (2022) 127100, https://doi.org/10.1016/j.biortech.2022.127100.

[17] J.L. Wagner, E. Jones, A. Sartbaeva, S.A. Davis, L. Torrente-Murciano, C.J. Chuck, V.P. Ting, Zeolite Y supported nickel phosphide catalysts for the hydrodenitrogenation of quinoline as a proxy for crude bio-oils from hydrothermal liquefaction of microalgae, Dalton Trans. 47 (2018) 1189–1201, https://doi.org/10.1039/c7dt03318d.

[18] Z. Bi, J. Zhang, E. Peterson, Z. Zhu, C. Xia, Y. Liang, T. Wiltowski, Biocrude from pretreated sorghum bagasse through catalytic hydrothermal liquefaction, Fuel 188 (2017) 112–120, https://doi.org/10.1016/j.algal.2018.05.012.

[19] Q. Ma, D. Chen, L. Wei, Q. Shen, Z. Ji, Y. Chen, X. Zou, C. Xu, J. Zhou, Bio-oil production from hydrogenation liquefaction of rice straw over metal (Ni, Co, Cu)-modified CeO_2 catalysts, Energy Sourc. Part A: Recov. Utiliz. Environ. Eff. 40 (2018) 200–206, https://doi.org/10.1080/15567036.2017.1409295.

[20] M.S. Seshasayee, P.E. Savage, Oil from plastic via hydrothermal liquefaction: production and characterization, Appl. Energy 278 (2020), 115673, https://doi.org/10.1016/j.apenergy.2020.115673.

[21] S. Hongthong, H.S. Leese, C.J. Chuck, Valorizing plastic-contaminated waste streams through the catalytic hydrothermal processing of polypropylene with lignocellulose, ACS Omega 5 (2020) 20586–20598, https://doi.org/10.1021/acsomega.0c02854.

[22] P. Zhao, Z. Yuan, X. Song, J. Zhang, A.J. Ragauskas, Product characteristics and synergy study on supercritical methanol liquefaction of lignocellulosic biomass and plastic, ACS Sustain. Chem. Eng. 9 (2021) 17103–17111, https://doi.org/10.1021/acssuschemeng.1c04289.

[23] T.M. Ukarde, H.S. Pawar, A Cu doped TiO2 catalyst mediated catalytic thermo liquefaction (CTL) of polyolefinic plastic waste into hydrocarbon oil, Fuel 285 (2021), 119155, https://doi.org/10.1016/j.fuel.2020.119155.

[24] M.S. Seshasayee, P.E. Savage, Synergistic interactions during hydrothermal liquefaction of plastics and biomolecules, Chem. Eng. J. 417 (2021), 129268, https://doi.org/10.1016/j.cej.2021.129268.

[25] A.P. Kumar, D. Depan, N. Singh Tomer, R.P. Singh, Nanoscale particles for polymer degradation and stabilization—Trends and future perspectives, Progr. Poly. Sci. 34 (2009) 479–515, https://doi.org/10.1016/j.progpolymsci.2009.01.002.

[26] R. Geyer, J.R. Jambeck, K.L. Law, Production, use, and fate of all plastics ever made, Sci. Adv. 3 (2017), https://doi.org/10.1126/sciadv.1700782.

[27] J.S. dos Passos, M. Glasius, P. Biller, Screening of common synthetic polymers for depolymerization by subcritical hydrothermal liquefaction, Proc. Saf. Environ. Protect. 139 (2020) 371–379, https://doi.org/10.1016/j.psep.2020.04.040.

[28] W.-T. Chen, K. Jin, N.-H. Linda Wang, Use of supercritical water for the liquefaction of polypropylene into oil, ACS Sustain. Chem. Eng. 7 (2019) 3749–3758, https://doi.org/10.1021/acssuschemeng.8b03841.

[29] J.S. dos Passos, S. Chiaberge, P. Biller, Combined hydrothermal liquefaction of polyurethane and lignocellulosic biomass for improved carbon recovery, Energy Fuel 35 (2021) 10630–10640, https://doi.org/10.1021/acs.energyfuels.1c01520.

[30] R. Mythili, P. Subramanian, D. Uma, Biofuel production from Prosopis juliflora in fluidized bed reactor, Energy Sourc. Part A: Recov. Utiliz. Environ. Eff. 39 (2017) 741–746, https://doi.org/10.1080/15567036.2016.1261205.

[31] A. Demirbas, Relationships between heating value and lignin, moisture, ash and extractive contents of biomass fuels, Energy Explor. Exploit. 20 (2002) 105–111, https://doi.org/10.1260/014459802760170420.

[32] J. Arun, K.P. Gopinath, P. SundarRajan, M. JoselynMonica, V. Felix, Co-liquefaction of *Prosopis juliflora* with polyolefin waste for production of high grade liquid hydrocarbons, Bioresour. Technol. 274 (2019) 296–301, https://doi.org/10.1016/j.biortech.2018.11.102.

[33] L. Atanda, S. Mukundan, A. Shrotri, Q. Ma, J. Beltramini, Catalytic conversion of glucose to 5-hydroxymethyl-furfural with a phosphated TiO2 catalyst, ChemCatChem 7 (2015) 781–790, https://doi.org/10.1002/cctc.201402794.

[34] Á.B. Sifontes, B. Gutierrez, A. Mónaco, A. Yanez, Y. Díaz, F.J. Méndez, L. Llovera, E. Cañizales, J.L. Brito, Preparation of functionalized porous nano-γ-Al2O3 powders employing colophony extract, Biotechnol. Reports 4 (2014) 21–29, https://doi.org/10.1016/j.btre.2014.07.001.

[35] G. Audisio, A. Silvani, P.L. Beltrame, P. Carniti, Catalytic thermal degradation of polymers: Degradation of polypropylene, J. Anal. Appl. Pyrolysis 7 (1984) 83–90, https://doi.org/10.1016/0165-2370(84)80042-X.

[36] D. Supramono, S. Lusiani, Improvement of bio-oil yield and quality in co-pyrolysis of corncobs and high density polyethylene in a fixed bed reactor at low heating rate, in: IOP Conference Series: Materials Science and Engineering, IOP Publishing, 162 (2016), pp. 012011.

[37] Y. Sakata, Catalytic degradation of polyethylene and polypropylene to fuel oil, Macromol. Symp. 135 (1998) 7–18, https://doi.org/10.1002/masy.19981350104.

[38] Eunyoung Hwang, JeongKun Choi, DoHee Kim, DaeWon Park, Heechul Woo, Catalytic degradation of polypropylene I. Screening of catalysts, Korean J. Chem. Eng. 15 (1998) 434–438.

[39] Y. Aray, D. Zambrano, M.H. Cornejo, E.V. Ludeña, P. Iza, A.B. Vidal, D.S. Coll, D. M. Jímenez, F. Henriquez, C. Paredes, First-principles study of the nature of niobium sulfide catalyst for hydrodesulfurization in hydrotreating conditions, J. Phys. Chem. C 118 (2014) 27823–27832, https://doi.org/10.1021/jp5059269.

[40] G.F. Leal, S. Lima, I. Graça, H. Carrer, D.H. Barrett, E. Teixeira-Neto, A.A. S. Curvelo, C.B. Rodella, R. Rinaldi, Design of nickel supported on water-tolerant Nb_2O_5 catalysts for the hydrotreating of lignin streams obtained from lignin-first biorefining, iScience 15 (2019) 467–488, https://doi.org/10.1016/j.isci.2019.05.007.

[41] D.P. Serrano, J. Aguado, J.M. Escola, Catalytic cracking of a polyolefin mixture over different acid solid catalysts, Ind. Eng. Chem. Res. 39 (2000) 1177–1184, https://doi.org/10.1021/ie9906363.

[42] Y. Chen, Y. Wu, R. Ding, P. Zhang, J. Liu, M. Yang, P. Zhang, Catalytic hydrothermal liquefaction of D. tertiolecta for the production of bio-oil over different acid/base catalysts, AICHE J. 61 (2015) 1118–1128, https://doi.org/10.1002/aic.14740.

[43] L. Dong, J. Xia, Y. Guo, X. Liu, H. Wang, Y. Wang, Mechanisms of caromatic-c bonds cleavage in lignin over NbOx-supported Ru catalyst, J. Catal. 394 (2021) 94–103, https://doi.org/10.1016/j.jcat.2021.01.001.

[44] A.M. Barrios, C.A. Teles, P.M. de Souza, R.C. Rabelo-Neto, G. Jacobs, B.H. Davis, L. E.P. Borges, F.B. Noronha, Hydrodeoxygenation of phenol over niobia supported Pd catalyst, Catal. Today 302 (2018) 115–124, https://doi.org/10.1016/j.cattod.2017.03.034.

[45] Q.N. Xia, Q. Cuan, X.H. Liu, X.Q. Gong, G.Z. Lu, Y.Q. Wang, $Pd/NbOPO_4$ multifunctional catalyst for the direct production of liquid alkanes from aldol adducts of furans, Angew. Chem. Int. Ed. 53 (2014) 9755–9760, https://doi.org/10.1002/anie.201403440.

[46] H. Jiao, X. Zhao, C. Lv, Y. Wang, D. Yang, Z. Li, X. Yao, Nb2O5-γ-Al_2O_3 nanofibers as heterogeneous catalysts for efficient conversion of glucose to 5-hydroxymethylfurfural, Sci. Report. 6 (2016) 34068.

[47] Y. Zhang, J. Wang, X. Li, X. Liu, Y. Xia, B. Hu, G. Lu, Y. Wang, Direct conversion of biomass-derived carbohydrates to 5-hydroxymethylfurural over water-tolerant niobium-based catalysts, Fuel 139 (2015) 301–307, https://doi.org/10.1016/j.fuel.2014.08.047.

[48] A. Kloekhorst, J. Wildschut, H.J. Heeres, Catalytic hydrotreatment of pyrolytic lignins to give alkylphenolics and aromatics using a supported Ru catalyst, Catal. Sci. Technol. 4 (2014) 2367–2377, https://doi.org/10.1039/C4CY00242C.

[49] B. Smutek, W. Kunz, F. Goettmann, Hydrothermal alkylation of phenols with alcohols in diluted acids, Comptes Rendus Chim. 15 (2012) 96–101, https://doi.org/10.1016/j.crci.2011.11.016.

[50] E. Laurent, B. Delmon, Deactivation of a sulfided NiMo/γ-Al_2O_3 during the hydrodeoxygenation of bio-oils. Influence of a high water pressure, Stud. Surf. Sci. Catal. 88 (1994) 459–466.

[51] R.F. Beims, Y. Hu, H. Shui, C. Xu, Hydrothermal liquefaction of biomass to fuels and value-added chemicals: products applications and challenges to develop large-scale operations, Biomass Bioenergy 135 (2020), 105510, https://doi.org/10.1016/j.biombioe.2020.105510.

[52] D. Xu, G. Lin, S. Guo, S. Wang, Y. Guo, Z. Jing, Catalytic hydrothermal liquefaction of algae and upgrading of biocrude: a critical review, Renew. Sust. Energ. Rev. 97 (2018) 103–118, https://doi.org/10.1016/j.rser.2018.08.042.

[53] A. Takagaki, J.C. Jung, S. Hayashi, Solid Lewis acidity of boehmite γ-AlO(OH) and its catalytic activity for transformation of sugars in water, RSC Adv. 4 (2014) 43785–43791, https://doi.org/10.1039/C4RA08061K.

[54] E. Laurent, B. Delmon, Influence of water in the deactivation of a sulfided NiMoγ-Al_2O_3 catalyst during hydrodeoxygenation, J. Catal. 146 (1994) 281–291, https://doi.org/10.1016/0021-9517(94)90032-9.